

# Synthesis and Cu(II) coordination of two new hexaamines containing alternated propylenic and ethylenic chains: Kinetic studies on pH-driven metal ion slippage movements

Manuel G. Basallote <sup>a,\*</sup>, Antonio Doménech <sup>b</sup>, Armando Ferrer <sup>a</sup>, Enrique García-España <sup>c,\*</sup>, José M. Llinares <sup>d</sup>, M. Angeles Máñez <sup>a</sup>, Conxa Soriano <sup>d</sup>, Begoña Verdejo <sup>c</sup>

<sup>a</sup> *Departamento de Ciencia de los Materiales e Ingeniería Metalúrgica, Facultad de Ciencias, Universidad de Cádiz, Apartado 40, Puerto Real, 11510 Cádiz, Spain*

<sup>b</sup> *Departamento de Química Analítica, Universidad de Valencia, C/Dr. Moliner 50, 46100 Burjassot, Valencia, Spain*

<sup>c</sup> *Instituto de Ciencia Molecular, Universidad de Valencia, Edificio de Institutos de Paterna, Apartado de Correos 22085, 46071 Valencia, Spain*

<sup>d</sup> *Instituto de Ciencia Molecular (ICMOL), Departamento de Química Orgánica, Facultad de Farmacia, Universidad de Valencia, Avda. Vicente Andrés Estellés s/n, 46100, Burjassot, Valencia, Spain*

Received 13 July 2005; received in revised form 23 January 2006; accepted 25 January 2006

Available online 6 March 2006

## Abstract

The synthesis of the open-chain and cyclic polyamines, 1,5,8,12,15,19-hexaazaheptadecane (L1) and 2,6,9,13,16,20-hexaaza[21]-(2,6)-pyridinophane (L2), are described. The protonation constants and interaction constants with Cu(II) have been determined by potentiometric measurements carried out at 298.1 K in 0.15 mol dm<sup>-3</sup> NaClO<sub>4</sub>. The values obtained are discussed as a function of the open-chain or cyclic nature of the ligands and compared with analogous polyamines containing different sets of hydrocarbon chains between the nitrogen donors. Kinetic studies on the acid-promoted dissociation of the Cu(II) complexes indicate that the mono and binuclear complexes of L1 decompose with different kinetics, a behavior unprecedented for open-chain polyamines. In contrast, the dissociation of the first metal ion is accelerated in the binuclear complexes of L2 and so, all the mono and binuclear complexes of L2 decompose with the same kinetics. The voltammetric response of Cu(II)–L1 and Cu(II)–L2 complexes has been studied in order to correlate electrochemical and structural data.

© 2006 Elsevier B.V. All rights reserved.

**Keywords:** Polyamines; Azamacrocycles; Protonation; Cu(II) coordination; Solution studies; Dissociation kinetics; Electrochemistry

## 1. Introduction

Polyamines constitute one of the categories of receptors most widely employed in coordination and supramolecular chemistry [1]. This broad interest stems from their versatility. Polyamine receptors can coordinate metal ions if the number of available amino groups is sufficient. On the other

hand, they can coordinate anions or dipolar species at pH values low-enough to allow extensive protonation of the amino groups. Different books and reviews cover this topic [2]. Within this field, we have prepared and studied the coordination capabilities of hexaamines of open-chain or cyclic nature containing different sets of ethylenic and propylenic chains between the amino groups (see Chart 1) [3–9]. In the cyclic compounds, the polyamine chains were attached through methylene groups to benzene or pyridine fragments. One of the main interests in the chemistry of these compounds stems from the fact that they form co-ordinatively unsaturated binuclear and mononuclear complexes.

\* Corresponding authors. Tel./fax: +34 963544879 (E. García-España).  
E-mail addresses: [manuel.basallote@uca.es](mailto:manuel.basallote@uca.es) (M.G. Basallote), [enrique.garcia-es@uv.es](mailto:enrique.garcia-es@uv.es) (E. García-España).

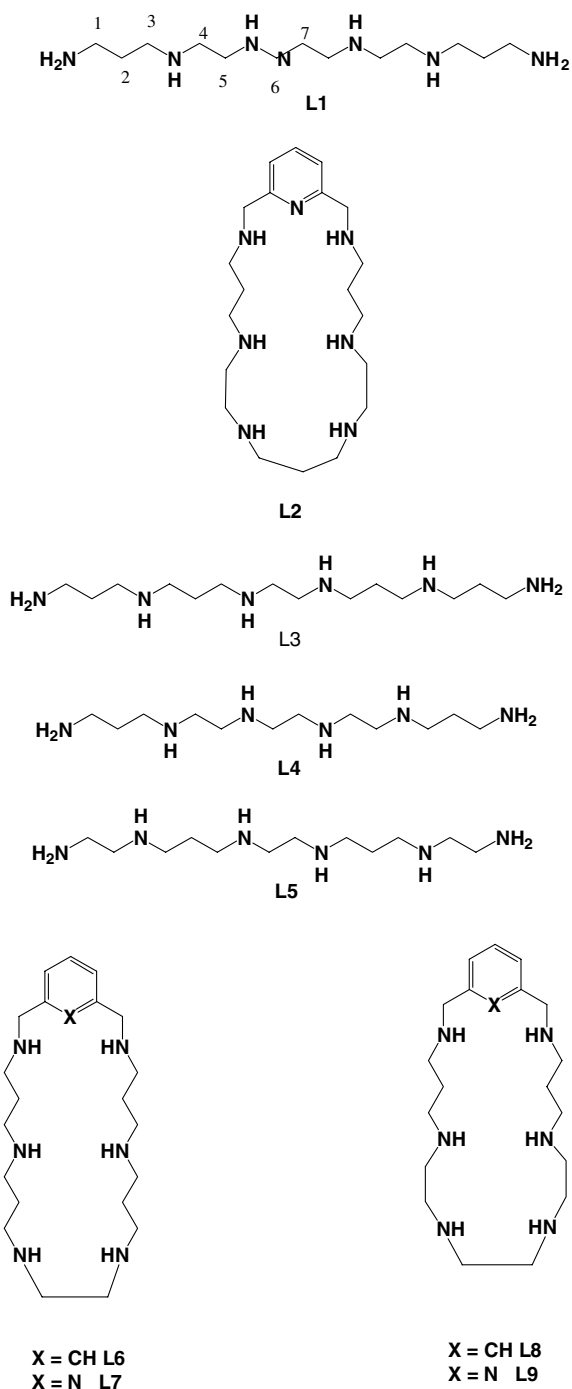


Chart 1.

In the case of the binuclear complexes, the number of nitrogen donors does not saturate the first coordination spheres of the metal ions leaving free positions that can be either vacant or occupied by ancillary ligands. Such ligands can be easily replaced by target molecules. Recently, we have communicated on the ability of the Cu(II) binuclear complexes of L7 (see Chart 1) to coordinate L-aspartate and L-glutamate amino acids as bridging ligands between the Cu(II) centers [6]. Another aspect of interest regards the mononuclear complexes of the cyclic ligands. In principle,

the stereochemical requirements of the metal ions do not match exactly with the conformational flexibility of the ligands, which is imposed by the aromatic fragment and the sequence of hydrocarbon chains in the polyamine bridges. This makes the mononuclear complexes to also have unsaturated coordination sites. The study of the complex decomposition kinetics has shown that the metal ions can, in some instances, reorganize the nitrogen atoms conforming its coordination sphere by breaking and re-making metal–nitrogen bonds as a function of the protonation degree and performing, therefore, a sort of hydrogen ion-driven molecular motion [5,7]. These slippage motions will be depending also on the basicity of the compound, which is marked by its open-chain or cyclic nature, and by the arrangement of hydrocarbon chains along the polyamine. The analysis of these simple movements can help to understanding more complex molecular movements occurring in living systems associated to pH gradients.

Among the compounds prepared, a polyamine containing a completely alternated sequence of propylenic and ethylenic chains was still lacking. In order to fill this gap, here we report on the synthesis of the open-chain polyamine 1,5,8,12,15,19-hexaazaheptadecane (L1) and on its related pyridinophane 2,6,9,13,16,20-hexaaza[21]-(2,6)-pyridinophane (L2). We analyze their acid–base behavior, Cu(II) coordination chemistry and their acid-promoted decomposition kinetics. In order to have further information about the slippage movements, we have also performed cyclovoltamperometric studies on these systems. We discuss on how the sequence of hydrocarbon chains affect free-energy terms and metal ion reorganizations in the compounds.

## 2. Results and discussion

### 2.1. Protonation behavior

The protonation constant of the ligands L1 and L2 calculated at 298.1 K in 0.15 mol dm<sup>-3</sup> NaClO<sub>4</sub> along with those previously reported for L3, L4, L5, L7 and L9 are presented in Table 1, while the distribution diagrams for L1 and L2 are collected in Fig. 1A and B.

The stepwise protonation constants obtained for L1 show high values for the first four protonation steps and intermediate values for the last two steps. The overall basicity is intermediate between those displayed by L3 and L4, which differ from L1 in having one more and one less propylenic chains, respectively (Chart 1).

Similarly to what happens for L3 and L4, L1 can bind four protons at nitrogen atoms which are not sharing ethylenic chains. Scheme 1 shows three possibilities for locating the protons filling this requirement. It is well established that such distributions of positive charges do not produce important repulsion yielding a high basicity [11,12]. However, the entry of the fifth proton necessarily leads to a situation in which two adjacent protons along an ethylenic chain should be protonated producing a drop in basicity ( $\log K_5 - \log K_6 = 2.16$ ).

Table 1  
Stepwise protonation constants for the protonation of polyamines L1 and L2 determined at 298.1 K in 0.15 mol dm<sup>-3</sup> NaClO<sub>4</sub>

Reaction	L1	L2	L3	L7	L4	L9	L5 <sup>c</sup>
L + H ⇌ HL <sup>a</sup>	10.26(1)	9.82(2) <sup>b</sup>	10.83(4)	10.67(1)	10.84(1)	10.04(2)	9.86(2)
HL + H ⇌ H <sub>2</sub> L	10.02(1)	9.38(2)	10.15(5)	9.85(1)	9.97(1)	9.43(2)	9.63(1)
H <sub>2</sub> L + H ⇌ H <sub>3</sub> L	9.17(1)	8.28(2)	9.30(4)	8.60(1)	8.99(1)	8.45(2)	8.65(1)
H <sub>3</sub> L + H ⇌ H <sub>4</sub> L	8.18(1)	7.35(2)	8.45(5)	7.49(1)	8.07(1)	7.53(2)	6.81(1)
H <sub>4</sub> L + H ⇌ H <sub>5</sub> L	6.02(1)	5.83(3)	7.30(5)	7.12(1)	5.91(2)	5.89(2)	5.90(1)
H <sub>5</sub> L + H ⇌ H <sub>6</sub> L	5.10(1)	4.66(4)	4.98(6)	4.99(2)	3.16(2)	2.83(3)	4.92(1)
log β	48.75	45.32	51.00	48.72	46.90	44.18	45.77

Values reported for L3 [3], L4 [4], L5 [10], L7 and L9 [5] are also included.

<sup>a</sup> Charges omitted for clarity.

<sup>b</sup> Values in parentheses are standard deviations in the last significant figure.

<sup>c</sup> Values determined at 298.1 K in 0.1 mol dm<sup>-3</sup> NMe<sub>4</sub>Cl.

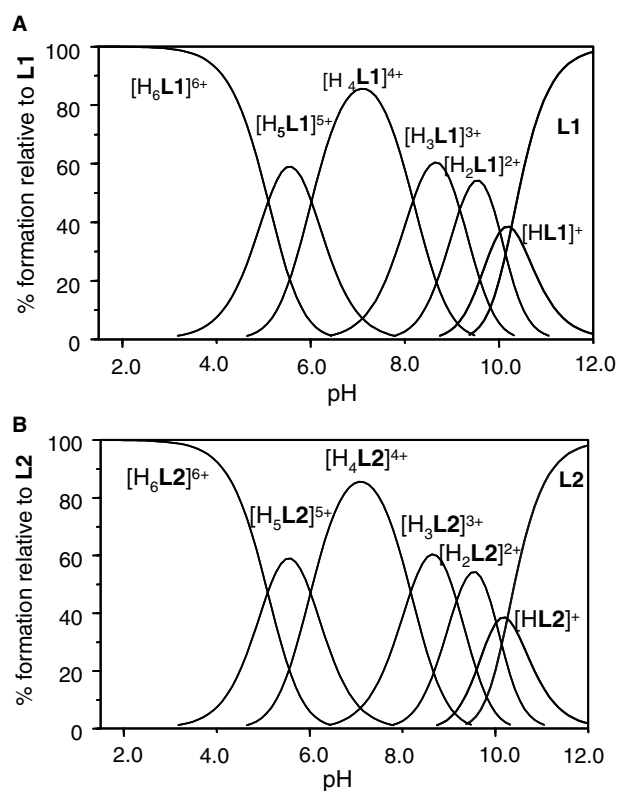
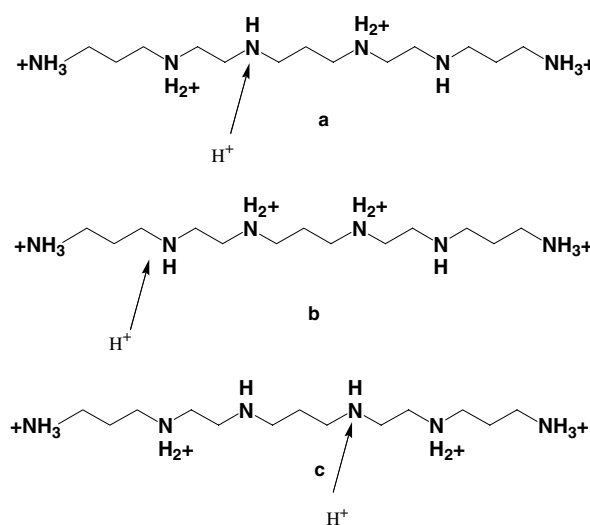


Fig. 1. Distribution diagrams for the systems H<sup>+</sup>-L1 and H<sup>+</sup>-L2.

Sixth protonation leads again to situations in which the incoming proton would be located between ammonium groups at distances of ethylenic and propylenic chains yielding a moderate decrease in basicity ( $\log K_5 - \log K_6 = 0.92$ ). The greater decrease in basicity observed for the last protonation of L4 ( $\log K_5 - \log K_6 = 2.75$ ) would be due to the binding of the proton in an amino group separated from its protonated neighbors only by ethylenic chains. A similar electrostatic analysis permits to explain the great difference between the constants for the fifth protonation steps of L1 and L3. Indeed, in L3 the first five protons can be added without sharing any ethylenic chains. Similar considerations account for the higher fourth protonation step of L1 with respect to L5 which also contains an alternated set of ethylenic and propylenic chains but with



Scheme 1. Schematic representation of three possible minimum energy situations for tetraprotonated L1. Arrows represent possible location for the entry of a fifth proton.

reverse order (Table 1). Fourth protonation in L5 will necessarily imply protons sharing the end of an ethylenic chain.

NMR spectroscopy can give interesting information regarding protonation sequences provided that the nitrogen atoms bearing the protons present different chemical environments [13–15]. Upon protonation, the carbon and proton nuclei experiencing the largest variations in chemical shift are those placed at two bond distances from the nitrogen atom being protonated; namely, the carbon nuclei placed in  $\beta$ -position and the hydrogen atoms attached to the  $\alpha$ -carbon atoms, which shift upfield and downfield, respectively. Fig. 2 collects the <sup>13</sup>C NMR spectra of L1 recorded at the pH values of predominance of the different protonated species.

All the assignments have been performed taking into account relevant bibliography and 2-D <sup>1</sup>H-<sup>1</sup>H and <sup>1</sup>H-<sup>13</sup>C correlation experiments (for the labeling, see Chart 1). The spectral variations shown in the <sup>13</sup>C NMR spectra (Fig. 2) and in the <sup>1</sup>H NMR spectra do not give clear indications for a net protonation pattern in L1. The signals of

carbon atoms C7 and C2 of the central methylene groups of the propylenic chains, which are, respectively, placed in  $\beta$  with respect to N1 and N2 and to N3, shift upfield throughout all the pH range where protonation occurs and therefore are little informative. The only difference would be the larger upfield shift experienced by carbon nuclei C2 ( $\Delta\delta = 5.12$  ppm) with respect to carbon nuclei C7 ( $\Delta\delta = 3.39$  ppm) on going from pD = 11.1 (spectrum F in Fig. 2) to pD = 6.71 (spectrum C in Fig. 2), thus suggesting that the first four protonations mainly affect the nitrogen atoms N1 and N2 in the external propylenic chains. The last two protonations will be involving at a larger extent the central propylenic chain (nitrogen N3) as suggested by the larger upfield shifts of signal C2 and C7 located in  $\beta$  with respect to the central nitrogen atoms. Nevertheless, the main indication provided by the NMR data is that protonation occurs randomly, thus meaning that the basicity of the different sites is close. However, as mentioned above, electrostatic arguments indicate that first protonation steps should not involve nitrogens belonging to the same ethylenic chain.

The overall basicity of cyclophane L2 is lower than that presented by its related open-chain polyamine L1 and intermediate between the basicity of the related pyridinophanes with one more propylenic chain (L7, 33233 set) and with one more ethylenic chain (L9, 32223 set). The reduced basicity of L2 with respect to L1 is due to moderate decreases in the basicity of all the protonation steps. The larger conformational freedom of the open-chain ligands permits to attain more easily anti conformations for all the chains when protonation occurs rendering more far apart the positive charges.

On the other hand, while the greater basicity of L7 with respect to L2 can be mainly attributed to the difference in basicity in the fifth protonation step, the greater basicity

of L2 with respect to L9 is mainly due to the larger sixth basicity constant of L2. Scheme 2 illustrates a likely protonation pattern for these stages. Again, it has to be emphasized that, with the exception of the last step, for all the others there are different prototypic isomers of close energy.

## 2.2. Metal ion coordination

The equilibrium constants determined by potentiometry in 0.15 mol dm<sup>-3</sup> NaClO<sub>4</sub> at 298.1 K for the formation of Cu(II) complexes of L1 and L2 are collected in Table 2, which also includes the values for the related open-chain polyamines L3 and L4 and pyridinophanes L7 and L9 for comparison.

Both polyamines, the open-chain hexaamine L1 and the pyridinophane L2 form mono- and binuclear complexes whose percentages of formation strongly depend on the Cu(II)–L molar ratio. Fig. 3 gathers, for instance, the distribution diagrams calculated for the system Cu(II)–L2 for mole ratios 2:1 and 1:1.

For the open-chain polyamine, we have detected a neutral mononuclear [CuL1]<sup>2+</sup> and two protonated species, [CuHL1]<sup>3+</sup> and [CuH<sub>2</sub>L1]<sup>4+</sup>. In the case of the cyclic ligand, an additional triprotonated species has also been detected. The values of the protonation constants of the neutral and monoprotinated species (entries 2 and 3 in Table 2) are very high for either the open-chain or cyclic polyamines supporting, therefore, that at least two nitrogens of the polyamine chain are not involved in the coordination to the metal. Moreover, the values of the formation constants of the [CuL]<sup>2+</sup> complexes compare well with those generally reported for open-chain tetraamines, suggesting four as a likely coordination number for these compounds [16].

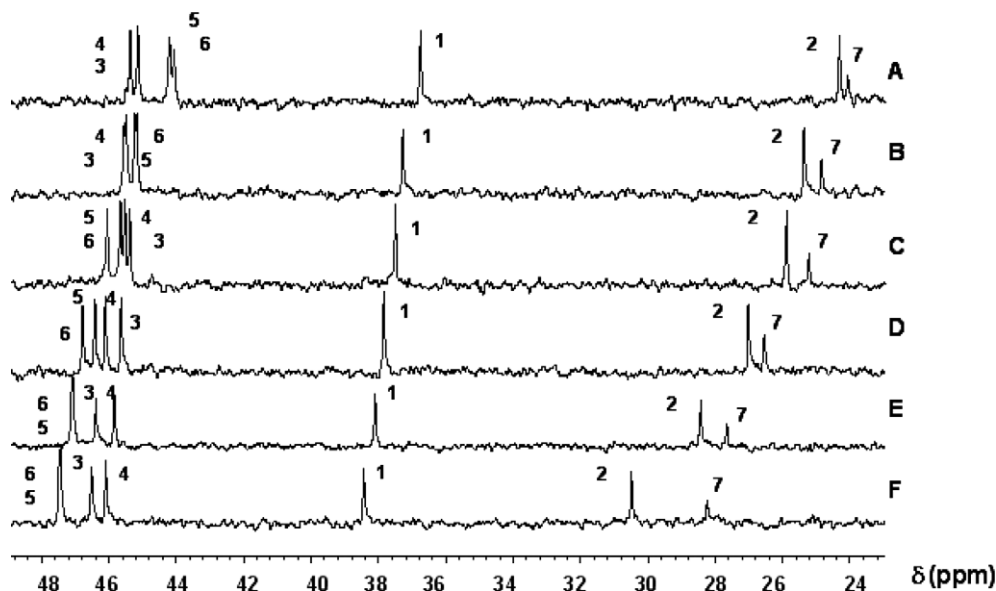
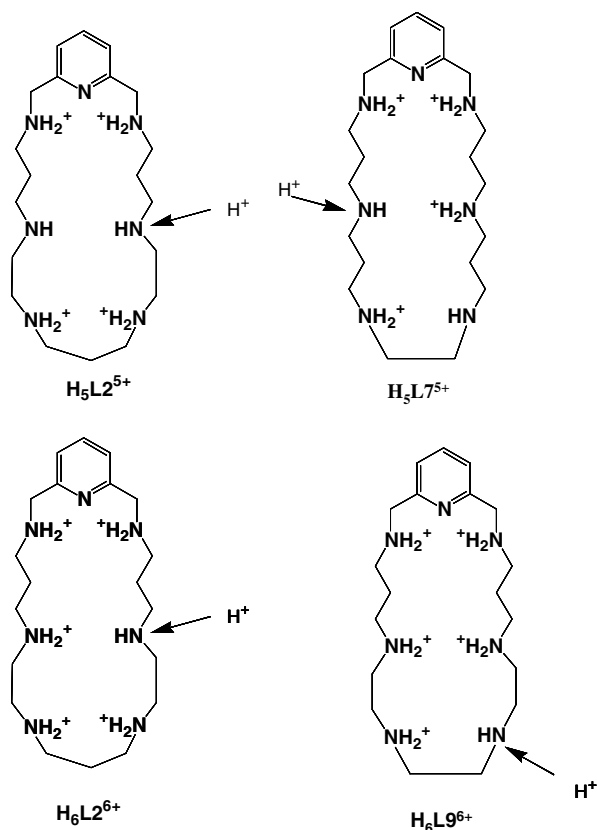


Fig. 2. <sup>13</sup>C NMR spectra in D<sub>2</sub>O of L1 recorded at (A) pD = 5.5; (B) pD = 6.7; (C) pD = 8.0; (D) pD = 9.0; (E) pD = 10.1 and (F) pD = 11.1.



Scheme 2. Likely protonation sites for the fifth and sixth protonation steps for pyridinophanes L2, L7 and L9.

In the case of the binuclear complexes, it is reasonable to assume that all the donor atoms in the ligands participate in the coordination. The additional pyridine nitrogen in the macrocyclic ligand will explain the higher formation constant for  $[Cu_2L_2]^{4+}$ .

One of the most interesting aspects of these complexes is to analyze how the different sequences of chelate rings affect the stability of the systems. To this respect, it has been postulated that the substitution of ethylene bridges by propylene ones in macrocyclic polyamines to give alternated sequences of 5- and 6-membered chelates favors the

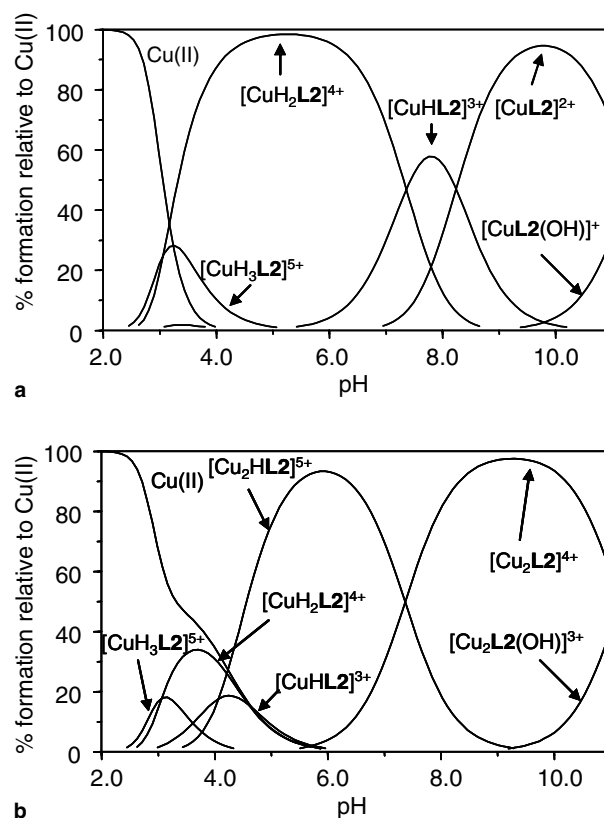


Fig. 3. Distribution diagram for the system  $Cu(II):L_2$ . (a)  $[Cu(II)] = [L_2] = 1 \times 10^{-3} \text{ mol dm}^{-3}$ . (b)  $[Cu(II)] = 2 \times 10^{-3} \text{ mol dm}^{-3}$ ,  $[L_2] = 1 \times 10^{-3} \text{ mol dm}^{-3}$ .

coordination of small ions like  $Cu(II)$  [17]. Inspection of the constants for the formation of the  $[CuL]^{2+}$  species shows for the open-chain polyamines the stability trend  $[CuL_4]^{2+} > [CuL_1]^{2+} > [CuL_3]^{2+}$ . The highest constant is achieved by the polyamine with two propylenic chains at the ends and a set of three consecutive ethylenic chains in the middle part of the molecule. The lowest constants are attained by the polyamine with the larger number of propylene chains. The situation for the cyclic amines is however quite different, the highest stability is achieved, in this case, by the macrocycle with the alternated sequence

Table 2

Logarithm of the stability constants for the interaction of L1 and L2 with  $Cu(II)$  determined in  $0.15 \text{ mol dm}^{-3} \text{ NaClO}_4$  at 298.1 K

Entry	Reaction	L1	L2	L3	L4	L7	L9
1	$Cu + L \rightleftharpoons CuL^a$	20.92(4) <sup>b</sup>	20.38(2)	19.35(4)	21.74(4)	18.34(3)	19.29(3)
2	$CuL + H \rightleftharpoons CuHL$	9.55(4)	8.24(2)	9.75(4)	10.06(3)	9.53(3)	9.64(3)
3	$CuHL + H \rightleftharpoons CuH_2L$	7.46(3)	7.35(2)	7.70(3)	6.60(1)	7.56(3)	6.71(2)
4	$CuH_2L + H \rightleftharpoons CuH_3L$		3.07(2)	4.06(1)	3.48(2)	4.65(2)	3.36(2)
5	$CuH_3L + H \rightleftharpoons CuH_4L$					4.69(2)	
6	$CuL + H_2O \rightleftharpoons CuL(OH) + H$		-11.34(4)				
7	$2Cu + L \rightleftharpoons Cu_2L$	28.80(2)	30.48(1)	27.17(3)		30.03(1)	30.21(2)
8	$Cu_2L + H \rightleftharpoons Cu_2HL$		4.08(6)			4.38(3)	4.63(3)
9	$CuL + Cu \rightleftharpoons Cu_2L$	7.88	10.10	7.82(4)		11.69(3)	10.92(5)
10	$2Cu + L + H_2O \rightleftharpoons Cu_2L(OH) + H$	20.48(4)	23.11(2)	19.37(5)	23.73(2)	22.26(2)	20.14(4)
11	$2Cu + L + 2H_2O \rightleftharpoons Cu_2L(OH)_2 + H$	9.72(5)	11.94(4)	10.02(10)		10.01	

The values for the formation of  $Cu(II)$  Complexes of L3, L4, L7 and L9 taken from Refs. [3–5] are also included.

<sup>a</sup> Charges omitted for clarity.

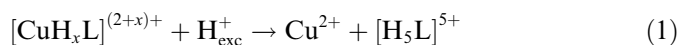
<sup>b</sup> Values in parentheses are standard deviations in the last significant figure.

of hydrocarbon chains in the bridge, while the lowest stability is observed for the macrocycle with the largest number of propylene chains L7. Plots of the logarithms of the stability constants against the overall basicity confirm the above sequences. It is interesting to emphasize that in none of the systems studied there is a macrocyclic effect. The relative flexibilities and stereochemical arrangements of these ligands should give rise to the different observed trends.

It is interesting to remark that, however, the binuclear complexes of the cyclic ligands present much closer values of stability between them. The implication of all nitrogen atoms including the pyridine nitrogens appears to balance the other effects.

### 2.3. Kinetics of decomposition of the Cu(II) complexes

The addition of an excess of acid to a solution of the Cu(II)–L complexes results in complex decomposition according to Eq. (1). The kinetics of these decomposition processes have been widely studied in the literature and we have recently shown that, in addition to the information about the decomposition process itself, it can also provide valuable information about the properties of the complex [5,7]



In particular, the observation of different kinetics of decomposition for the different  $[\text{CuH}_x\text{L}]^{(2+x)+}$  species indicates that the coordination mode of the ligand changes from a species to the other, thus revealing the existence of a pH-driven slippage of the metal ion through the macrocyclic cavity [5]. The existence of such movements was demonstrated for several macrocyclic ligands containing the 33233 or the 32223 polyamine units and it was proposed that the changes in the ligand coordination mode for different  $[\text{CuH}_x\text{L}]^{(2+x)+}$  species arise because the addition or removal of a proton to an uncoordinated amino group may introduce important changes in the electrostatic repulsions with the metal center. As these repulsions are expected to be very sensitive to the nature of the macrocyclic ligand, it was considered of interest to carry out a kinetic study of the decomposition process for the Cu(II) complexes with the ligands L1 and L2.

For the case of the open-chain L1 ligand, the species distribution curves indicate that the decomposition of the  $[\text{CuH}_2\text{L}]^{4+}$ ,  $[\text{CuHL}]^{3+}$  and  $[\text{CuL}]^{2+}$  can be studied by changing the pH of a starting solution containing Cu(II) and L1 in 1:1 molar ratio. However, the stopped-flow studies indicate that the kinetics of decomposition is the same for all the three species, the process occurring with a single kinetic step whose rate constant ( $k_{\text{obs}}$ ) changes with the acid concentration according to Eq. (2) with  $a = 2.1 \pm 0.4 \text{ s}^{-1}$ ,  $b = 7.4 \pm 0.9 \text{ s}^{-1}$  and  $c = 33 \pm 18 \text{ M}^{-1}$  (see Fig. 4)

$$k_{\text{obs}} = \frac{a + bc[\text{H}^+]}{1 + c[\text{H}^+]} \quad (2)$$

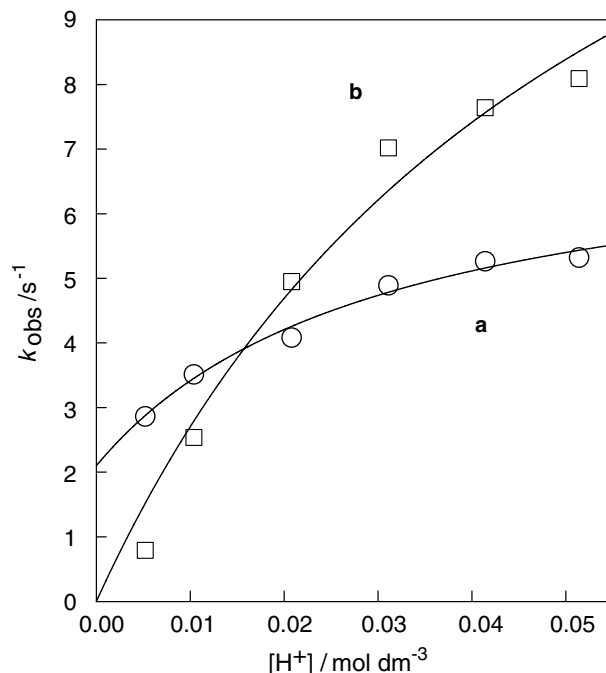


Fig. 4. Plot of the dependence with the acid concentration of the observed rate constant for the acid-promoted decomposition of the Cu(II) complexes with the L1 ligand. The circles and the squares correspond to the decomposition of the mono and binuclear complexes, respectively.

The observation of the same kinetics for the three species can be easily interpreted by considering that upon addition of an acid excess to a solution containing  $[\text{CuHL}]^{3+}$  or  $[\text{CuL}]^{2+}$ , they are converted to  $[\text{CuH}_2\text{L}]^{4+}$  within the mixing time of the stopped-flow instrument (ca. 1.7 ms), and it is the kinetics of decomposition of this species (or the more proton-rich  $[\text{CuH}_3\text{L}]^{5+}$ ) that is actually monitored in all cases. On the other hand, the rate law in Eq. (2) is usually interpreted according to the classical mechanism proposed by Margeum (Eqs. (3)–(5)) in which the breaking of the Cu–N bond occurs through the parallel attacks of  $\text{H}^+$  and  $\text{H}_2\text{O}$  to an activated  $(\text{Cu–N})^*$  species that contains a partially broken Cu(II)–N bond [18]. The rate law derived for this mechanism (Eq. (6)) coincides with Eq. (2) with the equivalences  $a = k_1 k_{\text{H}_2\text{O}} / (k_{-1} + k_{\text{H}_2\text{O}})$ ,  $b = k_1$  and  $c = k_{\text{H}} / (k_{-1} + k_{\text{H}_2\text{O}})$ , so that the values of  $k_1 = 7.4 \text{ s}^{-1}$  and  $k_{\text{H}} / k_{\text{H}_2\text{O}} = 33 \text{ M}^{-1}$  can be obtained from the values of  $a$ ,  $b$ , and  $c$



$$k_{\text{obs}} = \frac{k_1 k_{\text{H}_2\text{O}} + k_1 k_{\text{H}} [\text{H}^+]}{k_{-1} + k_{\text{H}_2\text{O}} + k_{\text{H}} [\text{H}^+]} \quad (6)$$

When the starting complex solution contains Cu(II) and L1 in 2:1 ratio, the decomposition of the  $[\text{Cu}_2\text{L}]^{4+}$ ,  $[\text{Cu}_2\text{L}(\text{OH})]^{3+}$  and  $[\text{Cu}_2\text{L}(\text{OH})_2]^{2+}$  can be studied, although the same kinetics is also observed for all the binuclear species. However, the experimental results in Fig. 4 indicate that the rate of decomposition of the binuclear complexes is

different from that of the mononuclear species and, although the data can also be fitted by Eq. (2), the values of  $a$ ,  $b$  and  $c$  are different. For the binuclear species,  $a$  is negligible,  $b = 18 \pm 4 \text{ s}^{-1}$  and  $c = 18 \pm 8 \text{ M}^{-1}$ . The observation of different kinetics of decomposition has been previously observed for mono and binuclear complexes of a given ligand [5,19,20], but this is to our knowledge the first case in which such differences are observed for a non-macrocyclic ligand. The differences in the kinetics indicate that decomposition of the binuclear species does not occur through the rapid release of one Cu(II) ion followed by the rate-determining decomposition of the resulting mononuclear species because in that case the kinetic parameters should be the same for all the species. Stopped-flow experiments carried out using the diode-array detector confirmed the absence of spectral changes within the mixing time of the stopped-flow, so that the experimental kinetic parameters correspond to the decomposition of the binuclear species. As the process occurs in a single kinetic step, the most plausible interpretation is to consider that the dissociation of both metal ions occurs with statistically controlled kinetics [21], a phenomenon previously observed for the decomposition of other binuclear Cu(II) complexes [19]. On the other hand, as the  $k_1$  value ( $=b$ ) for the binuclear complexes is higher than for the mononuclear species, this indicates that the Cu–N bonds are more labile in the binuclear complexes, which can be considered as an evidence of a more strained structure [22], probably caused by the electronic and steric constraints imposed by the simultaneous coordination of two metal ions.

For the case of the macrocyclic ligand L2, the kinetics of complex decomposition could be studied starting from each one of the  $[\text{CuH}_2\text{L}]^{4+}$ ,  $[\text{CuL}]^{2+}$  and  $[\text{Cu}_2\text{L}]^{4+}$  complexes; the other species detected in the potentiometric studies could not be studied because they always exist in equilibrium with significant amounts of other species and so, a separate analysis of their kinetic properties is not possible. In any case, all the L2 complexes studied decompose with the same kinetics (Fig. 5) and the values of the observed rate constant change linearly with the concentration of acid (Eq. (7) with  $k = 91 \pm 3 \text{ M}^{-1} \text{ s}^{-1}$ ). Thus, the kinetic results indicate that the Cu(II) complexes of L2 do not show the pH-driven slippage of the metal ion previously described [5] for the related complexes

$$k_{\text{obs}} = k[\text{H}^+]. \quad (7)$$

Although Eq. (7) can be considered a simplification of Eq. (2), the absence of terms different from the product  $b \times c$  ( $=k$ ) precludes the determination of any of the mechanistically relevant parameters as  $k_1$  or the quotient  $k_{\text{H}}/k_{\text{H}_2\text{O}}$ . However, the most important observation is that whereas the spectrum of solutions containing  $[\text{Cu}_2\text{L}]^{4+}$  displays a band centered at 670 nm, the initial spectrum recorded in the stopped-flow experiments shows the band at 590 nm typical of the mononuclear species. These results indicate that the cyclic nature of the L2 ligand makes the repulsion between the metal centers in the binuclear species more important than in the complexes with the related open-

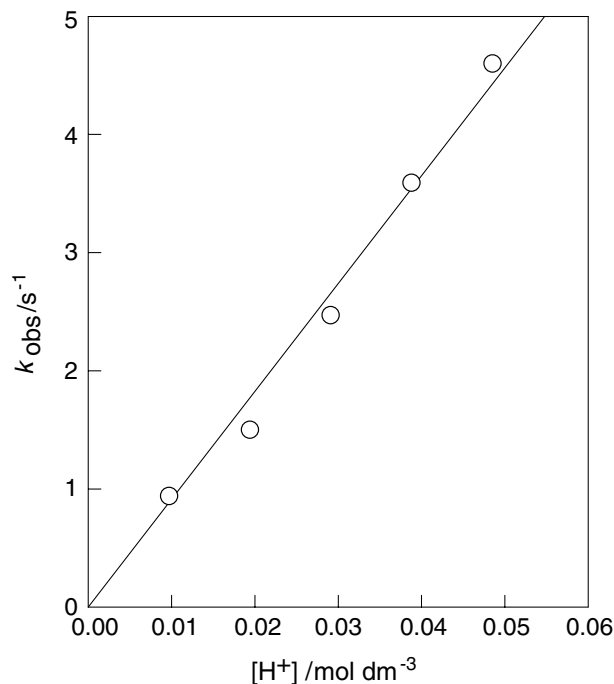


Fig. 5. Plot of the dependence with the acid concentration of the observed rate constant for the acid-promoted decomposition of the Cu(II) complexes with the L2 ligand.

chain L1 ligand, so that dissociation of the first metal ion now occurs during the mixing time of the instrument and the kinetic traces only give information about the much slower release of the second Cu(II) center. It is important to note that a similar very rapid release of the first metal ion has been previously observed for the binuclear complexes of the related pyridinophane with the 32223 polyamine (L9) [5], whereas the complexes of the 33233-containing pyridinophane (L7) decompose with statistically controlled kinetics, i.e., the rate of dissociation of the first metal ion only doubles the rate of the second one. Thus, the kinetic results in the present work indicate that the difficulties to accommodate two metal ions in the macrocyclic cavity are maintained when the size of the polyamine increases from 32223 (L9) to 32323 (L2) and, as a consequence, the binuclear complexes are strained and dissociation of the first metal ion is accelerated. However, a new increase in the size of the macrocycle (33233 polyamine, L7 ligand) leads to binuclear complexes in which both metal ions are so well accommodated that they behave independently of each other and their relative rates of dissociation are only controlled by the statistics. It is interesting to note that the conclusions derived from the kinetic data are also in agreement with the equilibrium results. The  $\log K$  values for the formation of  $[\text{Cu}_2\text{L}]^{4+}$  from  $[\text{CuL}]^{2+}$  and Cu(II) are 10.92, 10.10 and 11.69 for the pyridinophanes with the chains 32223 (L9), 32323 (L2) and 33233 (L7), respectively; i.e., the coordination of a second metal ion is more favored thermodynamically for the cycle with the 33233 sequence. In addition, the kinetic data indicate that this higher stability must also be associated with a less

strained structure that makes dissociation of both metal ions to occur at comparable rates (2:1 ratio). In agreement with this conclusion, the  $\log K$  values for the formation of the  $\text{Cu}_2\text{L}$  complexes with the polyamines containing the chains 32323 and 33233 (7.88 and 7.82, respectively) are significantly smaller than for the corresponding pyridinophanes and this results in more strained structures that lead to the very rapid release of one of the  $\text{Cu(II)}$  ions upon addition of an excess of acid.

#### 2.4. Electrochemical response

In Fig. 6a, a cyclic voltammetric experiment is presented for a  $1.0 \times 10^{-3} \text{ mol dm}^{-3}$  solution of  $\text{Cu(II)}$  plus  $0.5 \times 10^{-3} \text{ mol dm}^{-3}$  L1 at pH 9.0. In the initial cathodic scan, reduction peaks at  $-0.45$  and  $-0.72$  V appear followed, in the subsequent anodic scan, by a well-defined oxidation peak at  $-0.66$  V and ill-defined overlapping anodic waves near to  $+0.15$  V. On restricting the applied potential to the region from 0 to  $-500$  mV, the reduction peak at  $-0.45$  V is accompanied by a weak anodic counterpart at  $-0.38$  V, denoting that such peaks correspond to a reversible reduction process. Variation of peak potential and peak current with the potential scan rate in the range between  $0.01$  and  $1 \text{ V s}^{-1}$  for that couple permits to describe it in terms of a reversible one-electron per Cu electron transfer preceded by a relatively slow reaction [23].

Since peak potentials and currents remain essentially pH-independent in the pH range between 4.0 and 10.0, the proposed mechanism does not involve rate-controlling proton transfer processes. In view of the recognized preference of  $\text{Cu(I)}$  for adopting tetrahedral geometries, it appears reasonable to assume that the electrochemical pathway involves a pre-organization reaction in which the parent  $\text{Cu(II)}\text{-L1}$  complex, having probably a square-pyramidal coordination, undergoes a coordinative arrangement in order to adopt a tetrahedral-like coordination. This pre-organization reaction probably involves the redistribution of protons in the polyamine chain, in agreement with the kinetic data.

The voltammetric response of  $1.0 \times 10^{-3} \text{ mol dm}^{-3}$   $\text{Cu(II)}$  plus  $1.0 \times 10^{-3} \text{ mol dm}^{-3}$  L1 solutions is depicted in Fig. 6b. Now, cyclic voltammograms consist of a two-electron almost-reversible couple with peak potentials of  $-0.78$  (cathodic) and  $-0.58$  V (anodic), preceded by an ill-defined cathodic wave at  $-0.45$  V. This voltammetry indicates that there is a fast comproportionation reaction between the parent  $\text{Cu(II)}\text{L1}$  complex and the deposit of Cu metal formed electrochemically on the electrode surface, so that the second electron-transfer step is enhanced at the expense of the first.

The cyclic voltammetric response of  $\text{Cu(II)}\text{-L2}$  complexes is shown in Fig. 6c, corresponding to a  $1.0 \times 10^{-3} \text{ mol dm}^{-3}$  solution of  $\text{Cu(II)}$  plus  $0.5 \times 10^{-3} \text{ mol dm}^{-3}$  L2 at pH 9.0. In the initial cathodic scan, two overlapping reduction peaks at  $-0.60$  and  $-0.75$  V appear whose anodic counterparts are entirely absent in the subsequent reverse scan. Here, only

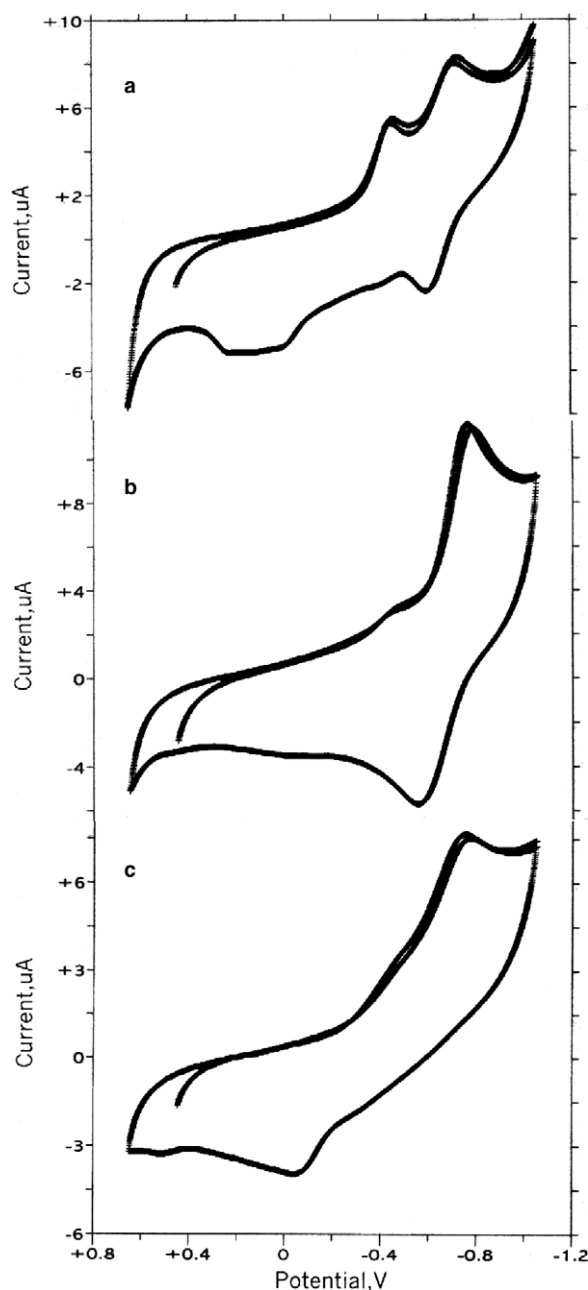


Fig. 6. Cyclic voltammograms of a  $1.0 \times 10^{-3} \text{ mol dm}^{-3}$  solution of  $\text{Cu(II)}$  plus: (a)  $0.5 \times 10^{-3} \text{ mol dm}^{-3}$  L1; (b)  $1.0 \times 10^{-3} \text{ mol dm}^{-3}$  L1; (c)  $1.0 \times 10^{-3} \text{ mol dm}^{-3}$  L2, all at pH 9.0. Potential scan rate  $0.050 \text{ V s}^{-1}$ .

one ill-defined oxidation wave near to  $-0.08$  V is recorded. This voltammetric response suggests that irreversible electron-transfer processes occur as a result of the inability of the parent metal complex for experiencing conformational changes required for a fast redox process.

### 3. Experimental

#### 3.1. Synthesis

Ligands L3–L9 have been prepared as described in Refs. [3–5,8,9]. 1,4,8,11-tetrazaundecane was purchased

from Aldrich (97% purity) and used without further purification.

### 3.1.1. 1,4,8,11-Tetrakis(*p*-tolylsulfonyl)-1,4,8,11-tetraazaundecane (**1**)

1,4,8,11-Tetraazaundecane (1.5 g, 9.4 mmol) dissolved in 250 cm<sup>3</sup> of THF and K<sub>2</sub>CO<sub>3</sub> (6.34 g, 45.9 mmol) dissolved in 100 cm<sup>3</sup> of water were placed in a three-necked round-bottomed flask provided with mechanical stirring. Then, a solution of *p*-tolylsulfonyl chloride (7.5 g, 40 mmol) in THF was dropwise added over 1 h. The solution was kept under stirring for one day, the organic phase was separated and vacuum evaporated to dryness. The residue was suspended in ethanol and refluxed for two more hours. Then, it was filtered and washed exhaustively with ethanol (Yield 82%); m.p. 61–63 °C. NMR:  $\delta_{\text{H}}$  (CDCl<sub>3</sub>): 1.94–2.03 (m, 2H), 2.40 (s, 6H), 2.42 (s, 6H), 3.11 (t, *J* = 7 Hz, 4H), 3.17 (b.s., 8H), 5.75 (t, *J* = 6 Hz, 2H), 7.28 (d, *J* = 7 Hz, 2H), 7.31 (d, *J* = 7 Hz, 2H), 7.65 (d, *J* = 8 Hz, 4H), 7.76 (d, *J* = 8 Hz, 4H).  $\delta_{\text{C}}$  (CDCl<sub>3</sub>): 21.5, 28.5, 43.4, 48.4, 50.3, 127.0, 127.3, 129.7, 129.9, 134.7, 136.8, 143.4, 143.8. MS *m/z* (FAB) 777 (M)<sup>+</sup>.

### 3.1.2. 1,18-Phthalimido-4,7,11,14-tetrakis(*p*-tolylsulfonyl)-4,7,11,14-tetraazaheptadecane (**2**)

The tosylated amine **1** (7.36 g, 9.5 mmol), K<sub>2</sub>CO<sub>3</sub> (29.7 g, 214.7 mmol) and *N*-(3-bromopropyl) phthalimide (5.1 g, 18.9 mmol) were suspended in refluxing CH<sub>3</sub>CN (300 cm<sup>3</sup>). After refluxing for 48 h, the suspension was filtered off. The solution was vacuum evaporated to dryness and the residue suspended in refluxing ethanol. Then, it was filtered to give **2** as a white solid (Yield 95%); m.p. 179–181 °C. NMR (CDCl<sub>3</sub>):  $\delta_{\text{H}}$  (ppm) 1.86–1.99 (m, 6H), 2.38 (s, 6H), 2.43 (s, 6H), 3.13–3.21 (m, 8H), 3.30–3.38 (m, 8H), 3.73 (t, *J* = 7 Hz, 4H), 7.29–7.33 (m, 8H), 7.67–7.74 (m, 8H), 7.80–7.83 (m, 8H).  $\delta_{\text{C}}$  (ppm) 21.5, 27.7, 28.5, 35.5, 48.1, 49.6, 50.2, 123.2, 127.3, 127.4, 129.9, 132.1, 133.9, 135.1, 135.2, 143.6, 168.2. MS *m/z* (FAB) 1150 (M)<sup>+</sup>.

### 3.1.3. 4,7,11,14-Tetrakis(*p*-tolylsulfonyl)-1,4,7,11,14,16-tetraazahexaazanadecane (**3**)

A mixture of compound **2** (5.1 g, 4.5 mmol) and hydrazine monohydrate 85% (2 cm<sup>3</sup>, 39.8 mmol) in THF (300 cm<sup>3</sup>) was refluxed for 24 h, then cooled and the resulting solid filtered off. After adding 50 cm<sup>3</sup> of water to form, the solution was vacuum evaporated to dryness to give a solid residue. The solid was dissolved in 100 cm<sup>3</sup> of CH<sub>2</sub>Cl<sub>2</sub> and the solution was dried with anhydrous Na<sub>2</sub>SO<sub>4</sub>. Then, it was vacuum evaporated to dryness to obtain **3** (Yield 86%). NMR (CDCl<sub>3</sub>):  $\delta_{\text{H}}$  (ppm) 1.65–1.72 (m, 2H), 1.90–2.00 (m, 4H), 2.38 (s, 6H), 2.42 (s, 6H), 3.10 (t, *J* = 7 Hz, 4H), 3.14 (t, *J* = 7 Hz, 4H), 3.16 (t, *J* = 7 Hz, 4H), 3.23–3.33 (m, 8H), 7.30 (d, *J* = 8 Hz, 4H), 7.31 (d, *J* = 8 Hz, 4H), 7.67 (d, *J* = 8 Hz, 4H), 7.69 (d, *J* = 8 Hz, 4H);  $\delta_{\text{C}}$  (ppm) 21.9, 28.9, 32.4, 39.1, 47.9, 48.0, 48.5, 49.3, 49.9, 127.6, 130.3, 130.2, 130.3. MS *m/z* (FAB) 891 (M)<sup>+</sup>.

### 3.1.4. 1,5,8,12,15,19-Hexakis(*p*-tolylsulfonyl)-1,5,8,12,15,19-hexaazanadecane (**4**)

**3** (2.8 g, 3.1 mmol) dissolved in 400 cm<sup>3</sup> of THF and K<sub>2</sub>CO<sub>3</sub> (1.74 g, 12.5 mmol) dissolved in 100 cm<sup>3</sup> of water were placed in a three-necked round-bottom flask provided with mechanical stirring. Then a solution of *p*-tolylsulfonyl chloride (1.2 g, 6.3 mmol) in THF was dropwise added over 1 h. The solution was kept under stirring for one day, the organic phase was separated and vacuum evaporated to dryness. The residue was suspended in ethanol and refluxed for two more hours. Then, it was filtered and washed exhaustively with ethanol (Yield 78%); m.p. 80–82 °C. NMR:  $\delta_{\text{H}}$  (CDCl<sub>3</sub>): 1.73–1.79 (m, 2H), 1.81–1.98 (m, 4H), 2.39 (s, 6H), 2.41 (s, 6H), 2.43 (s, 6H), 2.95 (t, *J* = 6 Hz, 4H), 3.14 (t, *J* = 7 Hz, 8H), 3.19–3.32 (m, 8H), 7.26 (d, *J* = 8 Hz, 8H), 7.30 (d, *J* = 8 Hz, 8H), 7.32 (d, *J* = 8 Hz, 4H), 7.67 (d, *J* = 8 Hz, 2H), 7.68 (d, *J* = 9 Hz, 2H), 7.69 (d, *J* = 9 Hz, 2H), 7.70 (d, *J* = 8 Hz, 2H).  $\delta_{\text{C}}$  (CDCl<sub>3</sub>): 21.5, 29.2, 40.4, 48.4, 49.7, 127.4, 127.7, 130.1, 130.4, 135.3, 135.5, 143.7, 144.2. MS *m/z* (FAB) 1197 (M)<sup>+</sup>.

### 3.1.5. 2,6,9,13,16,20-Hexakis(*p*-tolylsulfonyl)-2,6,9,13,16,20-hexaaza-[21]-(2,6)-pyridinophane (**5**)

**4** (3.1 g, 2.6 mmol) and K<sub>2</sub>CO<sub>3</sub> (3.6 g, 26 mmol) were suspended in refluxing CH<sub>3</sub>CN (250 cm<sup>3</sup>). To this mixture, 2,6-bis(bromomethyl)pyridine (0.7 g, 2.6 mmol) in 150 cm<sup>3</sup> of CH<sub>3</sub>CN was added dropwise over 2 h. The suspension was refluxed for further 20 h and then filtered off. The solution was vacuum evaporated to dryness and the residue suspended in refluxing ethanol. Then, it was filtered to give a white solid (Yield 76%); m.p. 99–101 °C. NMR;  $\delta_{\text{H}}$  (CDCl<sub>3</sub>) 1.68–1.76 (m, 4H), 1.80–1.87 (m, 2H), 2.36 (s, 6H), 2.40 (s, 6H), 2.43 (s, 6H), 3.01 (t, *J* = 7 Hz, 4H), 3.09 (t, *J* = 7 Hz, 4H), 3.11 (s, 8H), 3.20 (t, *J* = 7 Hz, 4H), 4.33 (s, 4H), 7.26 (t, *J* = 6 Hz, 9H), 7.32 (d, *J* = 8 Hz, 6H), 7.58 (d, *J* = 8 Hz, 4H), 7.64 (d, *J* = 8 Hz, 4H), 7.67 (d, *J* = 8 Hz, 4H).  $\delta_{\text{C}}$  (CDCl<sub>3</sub>) 21.5, 27.9, 47.0, 47.9, 48.6, 49.1, 54.1, 121.4, 127.2, 127.3, 129.8, 129.9, 135.0, 143.4, 143.7. MS *m/z* (FAB) 1301 (M)<sup>+</sup>.

### 3.1.6. 1,5,8,12,15,19-Hexaazanadecane (L1 · 6HBr) (**6**)

The tetratosylated amine **3** (4.4 g, 5.0 mmol) and phenol (23.8 g, 250 mmol) were suspended in HBr–AcOH 33% (250 cm<sup>3</sup>). The mixture was stirred at 90 °C for 24 h and then cooled; the resulting solid was filtered off and washed several times with CH<sub>2</sub>Cl<sub>2</sub> to give L1 · 6HBr (Yield 81%); m.p. 209–211 °C. NMR (D<sub>2</sub>O):  $\delta_{\text{H}}$  (ppm) 2.07–2.25 (m, 6H), 3.13 (t, *J* = 8 Hz, 4H), 3.24–3.31 (m, 8H), 3.52 (s, 8H);  $\delta_{\text{C}}$  (ppm) 23.1, 24.1, 36.8, 43.4, 45.3, 45.5. Anal. Calc. for C<sub>13</sub>H<sub>34</sub>N<sub>6</sub> · 6HBr: C, 20.5; H, 5.3; N, 11.6. Found: C, 21.2; H, 5.5; N, 10.8%.

### 3.1.7. 2,6,9,13,16,20-Hexaaza-[21]-(2,6)-pyridinophane hexahydrobromide trihydrate (L2 · 6HBr · 3H<sub>2</sub>O) (**7**)

The tosyl groups were removed as described for **6** (Yield 96%); m.p. 205–207 °C. NMR;  $\delta_{\text{H}}$  (D<sub>2</sub>O) 2.25 (q, 2H), 2.32–2.42 (m, 4H), 3.33–3.44 (m, 12H), 3.56–3.65 (m, 8H), 4.50

(s, 4H), 7.47 (d,  $J = 8$  Hz, 2H), 7.94 (t,  $J = 8$  Hz, 1H).  $\delta_{\text{C}}$  ( $\text{D}_2\text{O}$ ) 22.6, 22.9, 42.7, 43.2, 44.5, 44.8, 44.9, 51.1, 123.1, 139.7, 150.8. *Anal. Calc.* for  $\text{C}_{20}\text{H}_{39}\text{N}_7 \cdot 6\text{HBr} \cdot 3\text{H}_2\text{O}$ : C, 26.69; H, 5.28; N, 9.90. Found: C, 26.6; H, 5.0; N, 10.3%.

### 3.2. NMR measurements

The  $^1\text{H}$  and  $^{13}\text{C}$  NMR spectra were recorded on a Bruker Advance AC-300 spectrometer operating at 299.95 MHz for  $^1\text{H}$  and at 75.43 for  $^{13}\text{C}$  and Bruker Advance AC-400 spectrometer operating at 399.95 MHz for  $^1\text{H}$  and at 175.43 for  $^{13}\text{C}$ . For the  $^{13}\text{C}$  NMR spectra, dioxane was used as a reference standard ( $\delta = 67.4$  ppm) and for the  $^1\text{H}$  spectra, the solvent signal.

Adjustments to the desired pH were made using drops of DCl or NaOD solutions. The pD was calculated from the measured pH values using the correlation,  $\text{pH} = \text{pD} - 0.4$  [24].

### 3.3. emf Measurements

The potentiometric titrations were carried out at  $298.1 \pm 0.1$  K using  $\text{NaClO}_4$   $0.15 \text{ mol dm}^{-3}$  as the supporting electrolyte. The experimental procedure (burette, potentiometer, cell, stirrer, microcomputer, etc.) has been fully described elsewhere [25]. The acquisition of the emf data was performed with the computer program PASAT [26]. The reference electrode was an Ag/AgCl electrode in saturated KCl solution. The glass electrode was calibrated as an hydrogen-ion concentration probe by titration of previously standardised amounts of HCl with  $\text{CO}_2$ -free NaOH solutions and determining the equivalent point by the Gran's method [27], which gives the standard potential,  $E^0$ , and the ionic product of water ( $\text{p}K_{\text{W}} = 13.73(1)$ ). The concentrations of the different metal ions employed were determined gravimetrically by standard methods.

The computer program HYPERQUAD [28] was used to calculate the protonation and stability constants. The pH range investigated was 2.5–10.5 and the concentration of the different anions and of L ranged from  $1 \times 10^{-3}$  to  $5 \times 10^{-3} \text{ mol dm}^{-3}$ . The different titration curves for each system (at least two) were treated either as a single set or as separated curves without significant variations in the values of the stability constants. Finally, the sets of data were merged together and treated simultaneously to give the final stability constants. The distribution diagrams were calculated using the program HYSS [29]. Moreover, several measurements were made both in formation and in dissociation (from acid to alkaline pH and vice versa) to check the reversibility of the reactions.

### 3.4. Kinetic experiments

The kinetics of decomposition of the Cu(II) complexes with the ligands L1 and L2 was studied at  $25.0^\circ\text{C}$  using an Applied Photophysics SX17MV stopped-flow spectrophotometer. The Cu(II):L ratio (1:1 or 2:1) and the pH

of the starting solutions of the metal complexes were selected from the species distribution curves so that the concentration for one of the complex species is maximum while maintaining low concentrations of the other ones. For this reason, only those species which represent at least 80% of the total ligand under some conditions were studied. The solutions of the starting complexes were mixed in the stopped-flow instrument with solutions containing an excess of  $\text{HClO}_4$ , the ionic strength of both solutions being adjusted to  $0.10 \text{ mol dm}^{-3}$  with  $\text{NaClO}_4$ . The decomposition of the L1 and L2 complexes was monitored at 280 and 290 nm, respectively. In all cases, the data for the acid-promoted decomposition of the complexes could be satisfactorily fitted by a single exponential using the software of the stopped-flow instrument. However, some experiments were also performed using a PDA.1 diode-array detector in order to obtain information about the spectral changes occurring during the stopped-flow experiments. The data from the diode-array experiments were analyzed with the program GLINT [30] and yielded rate constants similar to those derived from the single-wavelength experiments, although the analysis also provides the spectrum of the reaction mixture immediately after the addition of the acid excess, which can be compared with the spectrum before addition of the acid (independently recorded with a Cary 50 UV-Vis spectrophotometer) to detect possible spectral changes occurring during the mixing time of the stopped-flow instrument.

### 3.5. Electrochemical measurements

Electrochemical measurements were performed in a three-electrode cell with BAS CV 50 W equipment using a BAS MF2012 glassy carbon working electrode (GCE) (geometric area  $0.071 \text{ cm}^2$ ), a platinum wire auxiliary electrode and a AgCl (3 M NaCl)/Ag reference electrode. The GCE was cleaned, polished, and activated as described elsewhere [31–33]. Electrochemical experiments were performed under argon atmosphere in solutions of  $\text{Cu}(\text{NO}_3)_2$  (Aldrich) in  $0.15 \text{ mol dm}^{-3}$   $\text{NaClO}_4$ , the pH being adjusted to the required value by adding the appropriate amounts of  $\text{HClO}_4$  and/or NaOH.

### Acknowledgments

Financial support from CTIDIB2002/244, Grupos S03/196, Junta de Andalucía (Group FQM-137) and DGICYT (Projects BQU2003-09215-CO3-01 and BQU2003-04737) (Spain) is gratefully acknowledged. J.M.Ll. thanks MCYT of Spain for a Ramón y Cajal contract. A.F. also thanks a grant from the joint program between Universidad de Cádiz (Spain) and Universidad de Oriente (Santiago, Cuba).

### References

- [1] A. Bianchi, M. Micheloni, P. Paoletti, *Coord. Chem. Rev.* 110 (1991) 17.

- [2] (a) J.-M. Lehn, *Angew. Chem. Int. Ed. Engl.* 27 (1988) 89;  
(b) J.-M. Lehn, *Supramolecular Chemistry. Concepts and Perspectives*, VCH, Weinheim, 1995;  
(c) F.P. Schdmidtchen, *Top. Curr. Chem.* 132 (1986) 101;  
(d) M.E. Huston, E.U. Akkaya, A.W. Czarnik, *J. Am. Chem. Soc.* 111 (1989) 8735;  
(e) B. Dietrich, *Pure Appl. Chem.* 65 (1993) 1457;  
(f) A. Bianchi, K. Bowman-James, E. Garcia-España, *Supramolecular Chemistry of Anions*, Wiley-VCH, New York, 1997;  
(g) P.D. Beer, *Acc. Chem. Res.* 31 (1998) 71;  
(h) P.D. Beer, J. Cadman, *Coord. Chem. Rev.* 205 (2000) 131;  
(i) P.D. Beer, P.A. Gale, *Angew. Chem. Int. Ed.* 40 (2001) 486;  
(j) P.A. Gale, *Coord. Chem. Rev.* 213 (2001) 79.
- [3] J.A. Aguilar, A. Bianchi, E. García-España, S.V. Luis, J.M. Llinares, J.A. Ramírez, C. Soriano, *J. Chem. Soc., Dalton Trans.* (1994) 637.
- [4] J. Aguilar, P. Díaz, F. Escartí, E. García-España, L. Gil, C. Soriano, B. Verdejo, *Inorg. Chim. Acta* 339 (2002) 307.
- [5] J. Aguilar, M.G. Basallote, L. Gil, M.A. Máñez, E. García-España, C. Soriano, B. Verdejo, *J. Chem. Soc., Dalton Trans.* (2004) 94.
- [6] B. Verdejo, J. Aguilar, A. Doménech, C. Miranda, P. Navarro, H.R. Jiménez, C. Soriano, E. García-España, *Chem. Commun.* (2005) 3086.
- [7] A. Mendoza, J. Aguilar, M.G. Basallote, L. Gil, J.C. Hernández, M.A. Máñez, E. García-España, C. Soriano, L. Ruiz-Ramírez, B. Verdejo, *Chem. Commun.* (2003) 3032.
- [8] J.A. Aguilar, E. García-España, J.A. Guerrero, S.V. Luis, J.M. Llinares, J.A. Ramírez, C. Soriano, *J. Chem. Soc., Chem. Commun.* (1995) 2237.
- [9] J.A. Aguilar, E. García-España, J.A. Guerrero, S.V. Luis, J.M. Llinares, J.A. Ramírez, C. Soriano, *Inorg. Chim. Acta* 246 (1996) 287.
- [10] A. Bencini, E. Berni, F. Chuburu, C. Giorgi, H. Handel, M. Le Baccon, P. Paoletti, B. Valtancoli, *Polyhedron* 21 (2002) 1459.
- [11] A. Bencini, A. Bianchi, E. García-España, M. Micheloni, J.A. Ramírez, *Coord. Chem. Rev.* 188 (1999) 97.
- [12] C. Frassinetti, L. Alderighi, P. Gans, A. Sabatini, A. Vacca, S. Ghelli, *Anal. Bioanal. Chem.* 376 (2003) 1041.
- [13] J.E. Sarnesky, H.L. Surprenant, F.K. Molen, C.N. Reilley, *Anal. Chem.* 47 (1975) 2116.
- [14] C. Frassinetti, S. Ghelli, P. Gans, A. Sabatini, M.S. Moruzzi, A. Vacca, *Anal. Biochem.* 231 (1995) 374.
- [15] (a) S.P. Dagnall, D.N. Hague, M.E. McAdam, *J. Chem. Soc., Perkin Trans. 2* (1984) 435;  
(b) S.P. Dagnall, D.N. Hague, M.E. McAdam, *J. Chem. Soc., Perkin Trans. 2* (1984) 1111;  
(c) D.N. Hague, A.D. Moreton, *J. Chem. Soc., Perkin Trans. 2* (1994) 265.
- [16] R.M. Smith, A.E. Martell, *NIST Stability Constants Database, Version 4.0*, National Institute of Standards and Technology, Washington DC, 1997.
- [17] B.P. Hay, R.D. Hancock, *Coord. Chem. Rev.* 212 (2001) 61.
- [18] R.A. Read, D.W. Margerum, *Inorg. Chem.* 20 (1981) 3143.
- [19] M.G. Basallote, J. Durán, M.J. Fernández-Trujillo, M.A. Máñez, *J. Chem. Soc., Dalton Trans.* (1999) 3817.
- [20] M.G. Basallote, J. Durán, M.J. Fernández-Trujillo, M.A. Máñez, M. Quirós, J.M. Salas, *Polyhedron* 20 (2001) 297.
- [21] R.G. Wilkins, *Kinetics and Mechanism of Reactions of Transition Metal Complexes*, second ed., VCH, Weinheim, 1991, pp. 18–23.
- [22] L.H. Chen, C.S. Chung, *Inorg. Chem.* 28 (1989) 1402.
- [23] R.S. Nicholson, I. Shain, *Anal. Chem.* 36 (1964) 706.
- [24] A.K. Covington, M. Paabo, R.A. Robinson, R.G. Bates, *Anal. Chem.* 40 (1968) 700.
- [25] E. García-España, M.J. Ballester, F. Lloret, J.M. Moratal, J. Faus, A. Bianchi, *J. Chem. Soc., Dalton Trans.* (1988) 101.
- [26] M. Fontanelli, M. Micheloni, in: *Proceedings of the I Spanish-Italian Congress on Thermodynamics of Metal Complexes*, Peñíscola, Castellón, 1990, Program for the automatic control of the microburette and the acquisition of the electromotive force readings.
- [27] (a) G. Gran, *Analyst (London)* 77 (1952) 661;  
(b) F.J. Rossotti, H. Rossotti, *J. Chem. Educ.* 42 (1965) 375.
- [28] P. Gans, A. Sabatini, A. Vacca, *Talanta* 43 (1996) 1739.
- [29] L. Alderighi, P. Gans, A. Ienco, D. Peters, A. Sabatini, A. Vacca, *Coord. Chem. Rev.* 184 (1999) 311.
- [30] GLINT Software, Applied Photophysics Ltd., Leatherhead, UK, 1997.
- [31] A. Doménech, J.V. Folgado, E. García-España, S.V. Luis, J.M. Llinares, J.F. Miravet, J.A. Ramírez, *J. Chem. Soc., Dalton Trans.* (1995) 541.
- [32] A. Doménech, E. García-España, V. Marcelino, B. Altava, S.V. Luis, J.F. Miravet, A. Bianchi, L. Ferrini, *Inorg. Chim. Acta* 252 (1996) 123.
- [33] A. Doménech, E. García-España, S.V. Luis, V. Marcelino, J.F. Miravet, *Inorg. Chim. Acta* 299 (2000) 238.